DMD Fast Forward. Published on September 15, 2017 as DOI: 10.1124/dmd.117.077883
This article has not been copyedited and formatted. The final version may differ from this version.

DMD # 77883

Title: Elucidation of the impact of P-glycoprotein and Breast Cancer Resistance Protein on the brain distribution of catechol-*O*-methyltransferase inhibitors

Author's name and affiliations:

Joana Bicker, Ana Fortuna, Gilberto Alves, Patrício Soares-da-Silva, Amílcar Falcão

Laboratory of Pharmacology, Faculty of Pharmacy, University of Coimbra, Pólo das Ciências da Saúde, Azinhaga de Santa Comba, 3000-548 Coimbra, Portugal (J.B., A.F., A.F.);

CNC – Center for Neuroscience and Cell Biology, University of Coimbra, 3004-517 Coimbra, Portugal (J.B., A.F., G.A., A.F.);

CICS-UBI – Health Sciences Research Centre, University of Beira Interior, Av. Infante D. Henrique, 6200-506 Covilhã, Portugal (G.A.);

Department of Research and Development, BIAL, Av. da Siderurgia Nacional, 4745-457, S. Mamede do Coronado, Portugal (P.S.d.S.);

Department of Pharmacology and Therapeutics, Faculty of Medicine, University of Porto, 4200-319 Porto, Portugal (P.S.d.S.).

DMD Fast Forward. Published on September 15, 2017 as DOI: 10.1124/dmd.117.077883
This article has not been copyedited and formatted. The final version may differ from this version.

DMD # 77883

Running title: P-gp and BCRP impact on the brain access of COMT inhibitors

Corresponding author:

Gilberto Alves, PharmD, Ph.D

Faculty of Health Sciences, CICS-UBI – Health Sciences Research Centre, University of Beira Interior, Av. Infante D. Henrique, 6200-506 Covilhã, Portugal

Phone: +351 275329002 / Fax: +351 275329099

E-mail address: gilberto@fcsaude.ubi.pt

Number of text pages: 27

Number of tables: 4

Number of figures: 4

Number of references: 61

Number of words in the Abstract: 242

Number of words in the Introduction: 746

Number of words in the Discussion: 1277

DMD Fast Forward. Published on September 15, 2017 as DOI: 10.1124/dmd.117.077883
This article has not been copyedited and formatted. The final version may differ from this version.

Non-standard abbreviations:

ABC, ATP-binding cassette; AUC_{extrap}, extrapolated area under the concentration-time curve; $AUC_{0\text{-}inf}$, area under the concentration-time curve from time zero to infinite; $AUC_{0\text{-}t}$, area under the concentration-time curve from time zero to the last measurable concentration; BBB, blood-brain barrier; BCRP, breast cancer resistance protein; $C_{last,}$ last observed concentration; C_{max}, maximum concentration; COMT, catechol-*O*-methyltransferase; DAD, diode-array detection; DDI, drug-drug interaction; EMA, European Medicines Agency; ER, efflux ratio; FDA, Food and Drug Administration; $f_{u,brain}$, unbound drug fraction in the brain; $f_{u,plasma}$, unbound drug fraction in plasma; HBSS, Hanks balanced salt solution; HPLC, high performance liquid chromatography; ITC, International Transporter Consortium; K_{el}, apparent elimination rate constant; K_p, ratio of total brain-to-plasma concentrations; $K_{p,uu}$, unbound brain-to-plasma ratio; $K_{p,uu,cell,pred}$, predicted unbound drug intracellular-to-extracellular partitioning coefficient; $K_{p,uu,cyto,pred}$, predicted unbound cytosolic-to-extracellular drug concentration ratio; $K_{p,uu,lyso,pred}$, predicted lysosomic-to-cytosolic unbound drug concentration ratio; MDCK, Madin-Darby Canine Kidney; MTT, [3-(4,5-dimethylthiazol-2-yl)-2,5-diphenyltetrazolium bromide]; Na-F, sodium fluorescein; Papp, apparent permeability coefficient; P-gp, P-glycoprotein; PBS, phosphate buffer saline; PEG, polyethylene glycol; MRT, mean residence time; TEER, transepithelial electrical resistance; $t_{1/2el}$, apparent terminal elimination half-life; t_{max}, time to achieve the maximum concentration; $V_{u,brain,pred}$, predicted volume of distribution of unbound drug in the brain.

DMD Fast Forward. Published on September 15, 2017 as DOI: 10.1124/dmd.117.077883
This article has not been copyedited and formatted. The final version may differ from this version.

Abstract

P-glycoprotein (P-gp) and breast cancer resistance protein (BCRP) are clinically important efflux transporters that act cooperatively at the blood-brain barrier, limiting the entry of several drugs into the CNS and affecting their pharmacokinetics, therapeutic efficacy and safety. In the present study, the interactions of catechol-*O*-methyltransferase (COMT) inhibitors (BIA 9-1059, BIA 9-1079, entacapone, nebicapone, opicapone and tolcapone) with P-gp and BCRP were investigated in order to determine the contribution of these transporters in their access to the brain. *In vitro* cellular accumulation and bidirectional transport assays were conducted in MDCK II, MDCK-MDR1 and MDCK-BCRP cells. *In vivo* pharmacokinetic studies were carried out for tolcapone and BIA 9-1079 in rats, with and without elacridar, a well-known P-gp and BCRP modulator. The results suggest that BIA 9-1079, nebicapone and tolcapone inhibit BCRP in a concentration-dependent manner. Moreover, with net flux ratios higher than 2 and decreased over 50 % in the presence of verapamil or Ko143, BIA 9-1079 was identified as P-gp substrate while BIA 9-1059, entacapone, opicapone and nebicapone revealed to be BCRP substrates. *In vivo,* brain exposure was limited for tolcapone and BIA 9-1079, although tolcapone crossed the blood-brain barrier in greater rate and extent than BIA 9-1079. The extent of brain distribution of both compounds was significantly increased in the presence of elacridar, attesting the involvement of efflux transporters. These findings provide relevant information and improve the understanding of the mechanisms that govern the access of these COMT inhibitors to the CNS.

DMD Fast Forward. Published on September 15, 2017 as DOI: 10.1124/dmd.117.077883
This article has not been copyedited and formatted. The final version may differ from this version.

Introduction

During preclinical drug development stages, it is essential to characterize the brain pharmacokinetics of new drug candidates and determine the rate and extent at which compounds are capable of crossing the blood-brain barrier (BBB) and reaching the central nervous system (CNS). This evaluation is relevant for CNS-active drugs and peripherally-active drugs, as potentially adverse side-effects can arise from an undesired brain exposure (Bungay *et al.*, 2015). Hence, a greater knowledge of general drug distribution to the brain will contribute to the adoption of drug design strategies that increase or restrict access through the BBB, thereby minimizing the risk of late stage failures and enhancing preclinical and clinical success. This may be achieved by combining the optimization of the intrinsic permeability of a compound with avoiding or targeting active efflux at the BBB (Cole *et al.*, 2012; Di *et al.*, 2013).

Often, the extrusion of xenobiotics out of the CNS, including therapeutic compounds and their metabolites, is performed by transporters from the ATP-binding cassette (ABC) family, namely P-glycoprotein (P-gp), breast cancer resistance protein (BCRP) and multidrug resistance-associated proteins (Löscher and Potschka, 2005). At the BBB, it has been shown that P-gp and BCRP work cooperatively to restrict the brain penetration of numerous compounds (Agarwal *et al.*, 2011; Römermann *et al.*, 2015), due to a broad substrate specificity and strategic location at the luminal membrane of brain endothelial cells (Bungay *et al.*, 2015). Additionally, it was found that the expression of BCRP is more prominent in humans than that of P-gp (Shawahna *et al.*, 2011), whereas P-gp is more abundantly expressed in rodents (Kamiie *et al.*, 2008; Uchida *et al.*, 2011). This reinforces the need of screening both transporters during CNS drug development, by identifying P-gp and BCRP substrates and inhibitors which could cause clinical drug-drug interactions (DDIs) and non-linear pharmacokinetics. *In vitro*

studies are recommended by the International Transporter Consortium (ITC), Food and Drug Administration (FDA) and European Medicines Agency (EMA) to identify substrates or inhibitors of clinically relevant ABC transporters involved in drug disposition at brain endothelium, including P-gp and BCRP (Giacomini *et al.*, 2010; European Medicines Agency, 2012; Food and Drug Administration, 2012).

The aim of the present work was to identify P-gp and BCRP substrates and/or inhibitors among catechol-*O*-methyltransferase (COMT) inhibitors and estimate the influence of these transporters on their CNS penetration. COMT inhibitors are used in combined therapy for the treatment of Parkinson's disease to improve the bioavailability and efficacy of L-DOPA (Gonçalves *et al.*, 2012; Kiss and Soares-da-Silva, 2014; Silva *et al.*, 2016). At the moment, there are three COMT inhibitors available in the market: entacapone; tolcapone, only used in patients unresponsive to other treatments and with monitoring of liver function; and opicapone, since its recent approval by EMA in June 2016 (Kiss and Soares-da-Silva, 2014; Annus and Vécsei, 2017). The peripheral (BIA 9-1059, BIA 9-1079, entacapone, opicapone) and/or central (nebicapone, tolcapone) enzymatic inhibition displayed by these compounds justify the investigation of the role that P-gp and/or BCRP may have in their access to the CNS (Learmonth *et al.*, 2002; Napolitano *et al.*, 2003; Parada and Soares-da-Silva, 2003; Kiss *et al.*, 2008; Bonifácio *et al.*, 2014).

Despite intensive research concerning *in vitro* BBB models, immortalized brain endothelial cell lines often exhibit paracellular leakiness caused by a defective formation of tight junctions, which renders them unsuitable for BBB permeability screens (Abbott *et al.*, 2014; Bicker *et al.*, 2014). Therefore, surrogate models are frequently applied to identify compounds that may interact with P-gp and BCRP at the BBB (Mahar Doan *et al.*, 2002; Wang *et al.*, 2005; Feng *et al.*, 2008; Hakkarainen *et*

al., 2010; Hellinger *et al.*, 2012; Chen *et al.*, 2013; Hu *et al.*, 2014), inclusively as screening tools in the pharmaceutical industry (Reichel, 2014). Consequently, *in vitro* cell-based assays were herein performed with Madin-Darby Canine Kidney (MDCK) type II cells as a surrogate BBB model, including stably transfected lines with *MDR1* (MDCK-MDR1) or *ABCG2* genes (MDCK-BCRP) of human origin. Intracellular accumulation assays were carried out to demonstrate transporter functionality and identify potential P-gp and BCRP inhibitors, while P-gp and BCRP substrates were identified resorting to validated bidirectional transport assays.

Lastly, *in vivo* studies were performed for BIA 9-1079, an active major metabolite of opicapone in rat, and for tolcapone, in order to determine and compare their extent of equilibration between plasma and brain and intra-brain distribution. Elacridar, a third-generation potent P-gp and BCRP modulator, was also co-administered to assess the impact of efflux inhibition on the brain distribution of these compounds.

Materials and methods

Chemicals and reagents

Reference compounds used in cell-based assays (carbamazepine, propranolol, trazodone, cimetidine, quinidine, sulfasalazine) were obtained from Sigma-Aldrich (St. Louis, MO, USA) with the exception of atenolol which was acquired from Acros Organics, ThermoFisher Scientific (MA, USA). Test compounds included BIA 9-1059, BIA 9-1079, entacapone, nebicapone, opicapone and tolcapone and were kindly supplied by BIAL-Portela & C^{a}., S.A. (S. Mamede do Coronado, Portugal). Their chemical structure is represented in Fig. 1. Acetonitrile (HPLC gradient grade), methanol (HPLC gradient grade) and DMSO were acquired from Fisher Scientific (Leicestershire, UK). Polyethylene glycol (PEG) was acquired from Merck Millipore

(Darmstadt, Germany). Sodium chloride 0.9 % solution and heparin-sodium 5.000 I.U/mL were purchased from B. Braun Medical (Queluz de Baixo, Portugal). All the remaining chemicals were from Sigma-Aldrich (St. Louis, MO, USA) unless otherwise stated.

Cell culture

MDCK II parent cells and transfected MDCK cells with human *MDR1* and *ABCG2* were obtained from the Netherlands Cancer Institute (NKI-AVL, Amsterdam, Netherlands). The cells were cultured in DMEM containing 0.04 M sodium bicarbonate and supplemented with 10 % heat-inactivated fetal bovine serum (Gibco Life Technologies, NY, USA), 100 µg/mL streptomycin and 100 I.U/mL penicillin. Cells were grown in T-75 flasks (Orange-Scientific, Belgium), passaged twice a week using a 0.25 % Trypsin-EDTA solution and cultured at 37 ºC in 5 % CO_2 and 95 % relative humidity. All assays were performed with MDCK II cells from passage 5–14, MDCK-MDR1 from passage 6–23 and MDCK-BCRP from passage 4–13. The cells were found to be negative for mycoplasma infection in periodic tests.

Cell viability studies

The influence of test compounds on cell viability was determined by the [3-(4,5-dimethylthiazol-2-yl)-2,5-diphenyltetrazolium bromide] (MTT) assay. MDCK II, MDCK-MDR1 and MDCK-BCRP cells were seeded into 96-well plates (Orange Scientific, Belgium) at a density of 1 x 10^4 cells per well and cultured for 24 h in a humidified incubator at 37 ºC in a 5 % CO_2 atmosphere. After removing the culture medium, 200 µL of fresh medium without (control cells) or with each compound at different concentrations was added to the wells and the cells were incubated for 4 h (5 to

100 μM) or 30 min (only 100 μM). Thereafter, the wells were washed twice with phosphate buffer saline (PBS) and the MTT solution (0.5 mg/mL) was added, followed by incubation for 2 h at 37 ºC in 5 % CO_2. Lastly, the MTT solution was removed and replaced with 100 μL of DMSO. Absorbance was measured at 570 nm with a reference wavelength of 620 nm on a Biotek Synergy HT microplate reader (Biotek Instruments®, VT, USA). Compound concentrations were not considered to compromise cell viability if it was maintained above 85 % compared to control cells (Li *et al.*, 2014).

Stability studies

Prior to intracellular accumulation and bidirectional transport assays, the stability of COMT inhibitors was evaluated in order to ensure drug preservation during these assays. Compound solutions were prepared in two concentrations corresponding to low (QC1) and high (QC3) quality control samples of the respective analytical calibration curve and data were compared before (reference sample) and after (stability sample) exposure to assay conditions (120 min maximum at 37 ºC in Hank's balanced salt solution (HBSS) with 10 mM HEPES pH 7.4). Compounds were considered stable under such conditions when the percentage of the ratio between stability and reference samples was maintained between 85–115 %.

Intracellular accumulation studies

To assess transporter functionality and identify P-gp and BCRP inhibitors, MDCK II, MDCK-MDR1 and MDCK-BCRP were seeded in 12-well plates (Corning Costar, NY, USA) at 3.0 x 10^5 cells per well for 48 h. The well-known P-gp or BCRP inhibitors, verapamil and Ko143 respectively, were used as positive controls. The assay was initiated by washing the cells twice with pre-warmed HBSS with 10 mM HEPES pH

7.4, followed by an incubation of 30 min in the absence (negative control, no inhibitor) or presence of verapamil (100 μM), Ko143 (0.5 μM) or test compound (100 μM in 0.1 % DMSO). Then, compound solutions were removed and the cells were incubated with 10 μM rhodamine-123 or Hoechst 33342 as P-gp or BCRP substrates, for 1 h at 37 ºC. Cellular accumulation of rhodamine-123 or Hoechst 33342 was stopped by washing the cells thrice with ice-cold PBS and cell lysis was performed with Triton X-100 (0.1 %, v/v) at room temperature during 30 min. An aliquot of cell lysate was used to measure the amount of accumulated rhodamine-123 or Hoechst 33342 utilizing the Biotek Synergy HT microplate reader (Biotek Instruments, VT, USA) in fluorescence mode (excitation and emission wavelengths of 485/528 nm for rhodamine-123; and 360/460 nm for Hoechst 33342). The protein content of cell lysates was also determined using the Bio-Rad Protein Assay Kit II (Bio-Rad Laboratories, California, USA) and cellular accumulation was normalized accordingly. When a significant P-gp or BCRP inhibition was observed ($p < 0.05$), additional concentrations of test compounds were evaluated to verify whether the inhibition was concentration-dependent, generate dose-response curves and determine the concentration of test compound that inhibits the accumulation of substrate by 50 % (IC_{50}).

Bidirectional transport studies

For bidirectional transport studies MDCK II, MDCK-MDR1 and MDCK-BCRP were seeded in 12-well polycarbonate microporous Transwell inserts (1.12 cm^2, 0.4 μm pore size; Corning Costar®, NY, USA) at a density of 6.0 x 10^5 cells per well. Assays were conducted 7 days post-seeding and culture medium was changed every other day. The transepithelial electrical resistance (TEER) of the polarized cell monolayer was monitored with the Evom® STX2 voltohmmeter (WPI, FL, USA). Sodium fluorescein

(Na-F) was used as a paracellular marker to attest the integrity of the cell monolayer during the transport assay and its fluorescence intensity was measured in a microplate reader, as described in the previous section.

Transport studies were performed from the apical to basolateral (AP-BL) and basolateral to apical (BL-AP) directions at 37 ºC with gentle shaking (45 rpm). Firstly, culture medium was replaced with pre-heated HBSS with 10 mM HEPES pH 7.4 and the cells were preincubated for 30 min at 37 ºC. Then, the donor solution containing the reference or test compound (0.1 % DMSO) was added to the apical (0.5 mL) or basolateral side (1.5 mL) and the receiver compartment was filled with fresh buffer. Aliquots (200 µL) were removed from the receiver side every 15 min during 60 min for high permeability compounds or every 30 min during 120 min for low permeability compounds. The removed volume was immediately replaced with fresh buffer to maintain compartment volumes and prevent the formation of a hydrostatic pressure gradient. At the end of the incubation period, aliquots were also withdrawn from the donor side to calculate mass balance.

The apparent permeability coefficient (Papp) of compounds was calculated following the equation (1) (Hubatsch *et al.*, 2007):

$$\text{Papp (cm/s)} = \frac{(dQ/dt)}{A \times C_0} \quad (1)$$

where dQ/dt is the rate of permeation, A is the surface area of the membrane (cm^2) and C_0 is the initial drug concentration in the donor compartment.

The efflux ratio (ER) for the BL-AP and AP-BL directions was determined by the equation (2):

$$\text{ER} = \frac{Papp_{BL-AP}}{Papp_{AP-BL}} \quad (2)$$

Net flux ratios were calculated by dividing the ER obtained in transfected cells by the ER obtained with the parent line MDCK II (Hu *et al.*, 2014). If a net flux ratio over 2

was observed, verapamil (100 µM, 30 min) or Ko143 (0.5 µM, 1 h) were added to both sides of the cell monolayer before the donor solutions, to confirm the specificity of P-gp or BCRP-mediated efflux.

Mass balance of each compound was calculated according to the equation (3):

$$\text{Mass balance} = \frac{C_f^D V^D + C_f^R V^R}{C_0^D V^D} \times 100 \quad (3)$$

where C_f is the final compound concentration in the donor (C_f^D) or receiver (Cf^R) compartment, C_0 is the initial concentration in the donor compartment and V^D and V^R are the volumes of the donor and receiver compartments, respectively (Hellinger *et al.*, 2012).

Animals

Healthy male Wistar rats weighting 275–300 g were purchased from Charles River Laboratories (L'Arbresle, France). The animals were housed in a controlled environment (12 h light/dark cycle; temperature 20 ± 2 °C; relative humidity 55 ± 5 %) for at least seven days prior to the beginning of the experiments, with *ad libitum* access to food and tap water. All experimental and care procedures were conducted in accordance with the European Directive (2010/63/EU) regarding the protection of laboratory animals used for scientific purposes and with the Portuguese law on animal welfare (Decreto-Lei 113/2013). The experimental procedures were reviewed and approved by the Portuguese National Authority for Animal Health, Phytosanitation and Food Safety (DGAV – Direção Geral de Alimentação e Veterinária).

In vitro brain and plasma protein binding

The unbound fraction of BIA 9-1079 and tolcapone in plasma ($f_{u,plasma}$) and brain homogenate ($f_{u,brain}$) were estimated by ultrafiltration, according to Fortuna et al.

(Fortuna *et al.*, 2013) with minor alterations. An Amicon® Ultra-0.5 centrifugal filter device was used, with a low binding regenerated cellulose membrane and a 30 KDa cut-off (Merck Millipore, Darmstadt, Germany). Blank plasma and homogenates of brain tissue collected from healthy Wistar rats (1 mL) were spiked with 10 µL of compound solution yielding a final concentration of 100 µM. Brain homogenates were prepared by dilution with 50 mM PBS pH 7.4 (1:4, w/v) using a Teflon® pestle tissue homogenizer (Thomas Scientific, Swedesboro, USA). At the beginning of the assay, 100 µL of plasma or brain homogenate were withdrawn to determine the initial compound concentration (C_1), while the remaining portion was incubated for 1 h at 37º C in a shaking water bath. Following the incubation period, 100 µL were collected to determine the concentration of test compound not subjected to ultrafiltration (C_t) and 500 µL were transferred to the ultrafiltration device (n = 4) and spun at 14000 g for 15 min at 37 ºC. Then, the concentration of compound was analysed in the ultrafiltrate (C_f), in the concentrated sample at the top of the ultrafiltration device (C_c) and in the remaining sample volume at the end of the experiment (C_{37}) by HPLC. The unbound fractions (f_u) in plasma and brain were calculated considering equation 4 (Fortuna *et al.*, 2013):

$$f_u = 1 - \frac{C_t - C_f}{C_t} \quad (4)$$

where C_t is the total concentration of compound not subjected to ultrafiltration and C_f is the ultrafiltrate free drug concentration. In order to correct for the brain tissue dilution that occurs during homogenization, $f_{u,brain}$ was estimated according to equation 5 (Hammarlund-Udenaes, 2014):

$$f_{u,brain} = \frac{1/D}{((1/f_u)-1)+1/D} \quad (5)$$

where f_u is the fraction of unbound drug in the diluted brain homogenate and D is the dilution factor of brain tissue. The recovery and stability of plasma and brain samples were calculated following equations 6 and 7 (Wang and Williams, 2013):

$$\% \text{ recovery} = \frac{(C_C \times V_C + C_f \times V_f)}{C_1 \times V_1} \quad (6)$$

$$\% \text{ stability} = \left(\frac{C_{37}}{C_1}\right) \times 100 \quad (7)$$

where C_1 is the initial compound concentration at the beginning of the assay, V_1 is the volume of plasma or brain homogenate loaded to the ultrafiltration device, C_C and V_C are the drug concentration and volume of the sample on the top of the ultrafiltration device at the end of the centrifugation, C_f and V_f are the drug concentration and volume of the ultrafiltrate and C_{37} is the drug concentration at the end of the experiment.

In vivo brain disposition of BIA 9-1079 and tolcapone

Rats were randomly distributed in two groups, each of which received either BIA 9-1079 (n = 30) or tolcapone (n = 27). On the day of the experiment, stock solutions of tolcapone and BIA 9-1079 were prepared in DMSO (40 mg/mL) and diluted 20-fold in a vehicle composed of PEG-NaCl 0.9 % (50:50, v/v) to achieve a final concentration of 2 mg/mL. Prior to administration, the animals were anesthetized by intraperitoneal administration of sodium pentobarbital (60 mg/kg). Under anaesthesia, the formulation of tolcapone or BIA 9-1079 was administered by an intravenous bolus injection into the lateral tail vein, at the dose of 10 mg/kg with a total volume of administration of 5 mL/kg. The dose used in this study was based on literature data (Funaki *et al.*, 1994) and on the requirement of clear solutions appropriate for intravenous administration, dependent on compound solubility. The intravenous route was selected in order to circumvent intestinal absorption and ensure 100 % bioavailability. For tolcapone, plasma and brain samples were collected immediately after its administration (0.03 h)

and at 0.08, 0.25, 0.5, 0.75, 1, 3, 6 and 12 h post-dosing; for BIA 9-1079, an additional sample collection was performed at 24 h post-dosing.

The blood was collected from the left ventricle by cardiac puncture using heparinized syringes and immediately transferred to heparinized tubes for centrifugation at 1514 g for 10 min at 4 °C. Intracardiac perfusion with NaCl 0.9 % was performed to remove residual blood from brain tissue. The brain was rapidly removed, carefully weighed and stored frozen at -80 °C until drug analysis.

To determine the influence of P-gp and/or BCRP in the transport of BIA 9-1079 and tolcapone, the rats were randomly divided into four groups (n = 8-12 animals per group), all of which received tolcapone or BIA 9-1079 in the same dose (10 mg/kg) of the previous study. In two of the groups, elacridar (2.5 mg/kg) was added to the formulation and co-administered with tolcapone or BIA 9-1079; on the other hand, the other two groups were co-administered with the vehicle [PEG-NaCl 0.9 % (50:50, v/v)] instead of elacridar. The animals were sacrificed at 0.08, 0.25, 0.5 and 1 h post-dosing and the blood and brain were collected using the aforementioned procedures.

Drug analysis

Samples collected from the bidirectional transport and protein binding assays, as well as plasma and brain samples from the *in vivo* studies were analysed by HPLC with a diode-array detector (DAD) in an integrated chromatograph model LC-2040C-3D (Shimadzu Corporation, Tokyo, Japan) using validated techniques. Chromatographic analysis was achieved in a LiChroCART® Purospher Star-C18 column (55 × 4 mm; 3 μm particle size from Merck Millipore, Darmstadt, Germany) by isocratic or gradient elution. Samples from cell-based assays were injected directly or following dilution with HBSS supplemented with 10 mM HEPES pH 7.4, whereas plasma and brain

samples of BIA 9-1079 and tolcapone were pre-treated according to published methods (Gonçalves *et al.*, 2013, 2016) with minor modifications. Tamoxifen (90 μg/mL) and nebicapone (35 μg/mL) were used as internal standards for plasma and brain samples, respectively. Chromatographic conditions and main validation parameters are summarized in Supplemental Table 1.

Statistical and pharmacokinetic data analysis

Data from *in vitro* studies were processed using Graphpad Prism® 5.03 (San Diego, CA, USA) and expressed as mean ± SD. An unpaired two-tailed Student's t test was used to determine the differences of cell viability (%) compared with untreated control cells (100 % cell viability) in the MTT assay and of rhodamine-123 or Hoechst 33342 accumulation compared with negative control cells (no inhibitor) in the intracellular accumulation assay. Differences were considered statistically significant when $*p < 0.05$, $**p < 0.01$ and $***p < 0.001$. IC_{50} values were calculated by non-linear regression generating sigmoid dose-response curves with variable slope, with the fitting method of least-squares.

The maximum concentration (C_{max}) in plasma and brain of tolcapone and BIA 9-1079 and the corresponding time to reach C_{max} (t_{max}) were directly obtained from the experimental data. The remaining pharmacokinetic parameters were estimated from the mean concentration values determined at each time point by non-compartmental analysis using the WinNonlin® version 6.4 software. The pharmacokinetic parameters evaluated were the area under the drug concentration time-curve (AUC) from time zero to the time of the last measurable drug concentration (AUC_{0-t}) which was calculated by the linear trapezoidal rule; the AUC from time zero to infinite (AUC_{0-inf}) was calculated from $AUC_{0-t} + (C_{last}/k_{el})$, where C_{last} is the last observed concentration and k_{el} is the

DMD Fast Forward. Published on September 15, 2017 as DOI: 10.1124/dmd.117.077883
This article has not been copyedited and formatted. The final version may differ from this version.

apparent elimination rate constant estimated by log-linear regression of the terminal segment of the concentration–time profile; the percentage of AUC extrapolated from t_{last} to infinity [$AUC_{extrap}(\%)$], where t_{last} is the time of C_{last}; and the apparent terminal elimination half-life ($t_{1/2el}$) and mean residence time (MRT).

The unbound ratio of brain-to-plasma concentrations ($K_{p,uu}$) was calculated from the ratio of AUC_{0-t} for total brain and plasma concentrations (K_p), $f_{u,plasma}$ and $f_{u,brain}$, using equation 8 (Fridén *et al.*, 2011; Loryan *et al.*, 2014):

$$K_{p,uu} = \frac{K_p}{\frac{1}{f_{u,brain\ corrected}} \times f_{u,plasma}} \quad (8)$$

where $f_{u,brain,corrected}$ values are $f_{u,brain}$ values corrected for lysosomal trapping using the pH partitioning model proposed by Fridén et al. (Fridén *et al.*, 2011). Other parameters such as the predicted unbound cytosolic-to-extracellular drug concentration ratio ($K_{p,uu,cyto,pred}$), the predicted lysosomic-to-cytosolic unbound drug concentration ratio ($K_{p,uu,lyso,pred}$), the predicted unbound drug intracellular-to-extracellular partitioning coefficient ($K_{p,uu,cell,pred}$) and the predicted volume of distribution of unbound drug in the brain ($V_{u,brain,pred}$) were also estimated according to Fridén et al. (Fridén *et al.*, 2011) and Loryan et al. (Loryan *et al.*, 2014).

Results

Cellular viability of MDCK II, MDCK-MDR1 and MDCK-BCRP cells

The MTT assay revealed a significant reduction on cell viability for BIA 9-1079, nebicapone and tolcapone after a 4 h incubation period, particularly at 100 µM. This was most evident for BIA 9-1079, for which a decrease of more than 15 % cell viability was observed at concentrations higher than or equal to 20 µM in MDCK-MDR1 cells ($p < 0.01$), 50 µM in MDCK-MDR1 ($p < 0.001$) and MDCK-BCRP cells ($p < 0.01$) and at

80 and 100 μM in all cell lines (p = 0.002 for MDCK II at 80 μM or < 0.001 in remaining cases). Concerning nebicapone, MDCK-MDR1 cells were affected at 80 μM ($p < 0.05$) and 100 μM ($p < 0.001$). Furthermore, a decrease was also observed for tolcapone at 50, 80 and 100 μM in MDCK-MDR1 cells ($p < 0.01$) and at 100 μM in MDCK-BCRP cells ($p < 0.01$). Hence, the incubation period was shortened to 30 min, the duration of the incubation period in intracellular accumulation assays, and no significant loss of cell viability ($p > 0.05$) was verified at 100 μM, in all cell lines. For studies exceeding 30 min (i.e. bidirectional transport assay) the selected concentration for these test compounds was 10 μM.

Stability of COMT inhibitors

During 120 min, stability at 37 ºC in HBSS with 10 mM HEPES pH 7.4 was kept in the range 85-115 % for all compounds with the exception of BIA 9-1079 (Supplemental Table 2), for which significant reductions of average stability values under 85 % were observed at lower concentrations (QC1) after 90 min. These results were taken into consideration when defining the maximal duration of subsequent assays, in association with data from the MTT studies.

Intracellular accumulation of rhodamine-123 and Hoechst-33342 in MDCK II, MDCK-MDR1 and MDCK-BCRP cells

As presented in Fig. 2A-B, the functionality of P-gp and BCRP was confirmed through a significantly lower uptake of rhodamine-123 and Hoechst 33342 in MDCK-MDR1 and MDCK-BCRP cells compared with the parent line MDCK II. The addition of a P-gp (100 μM verapamil) or BCRP inhibitor (0.5 μM Ko143) reversed this tendency and led to an increased accumulation of classic substrates (rhodamine-123 and Hoechst

33342) in both cases (by 3.0 and 4.2-fold, respectively). In contrast, as expected, no inhibitory effect was observed in MDCK II cells.

Incubation of MDCK-MDR1 and MDCK-BCRP cells with 100 μM test compounds revealed a significant accumulation of rhodamine-123 or Hoechst 33342 for some compounds in relation to negative controls (no addition of inhibitor) (Fig. 2C-D). Since BIA 9-1079 significantly inhibited P-gp in MDCK-MDR1 cells, additional concentrations were tested, detecting a concentration-dependent inhibition. Nevertheless, the IC_{50} of BIA 9-1079 could not be experimentally determined because it would be necessary to test concentrations over 100 μM to reach the top inhibition plateau, which would compromise solubility and the accuracy of the results. In MDCK-BCRP cells, further concentrations of BIA 9-1079, nebicapone and tolcapone (Fig. 3A-C) were tested, as a very significant BCRP inhibition was observed at 100 μM (Fig. 2D). The lowest IC_{50} value was obtained for BIA 9-1079 (IC_{50} = 3.85 ± 1.0 μM), followed by nebicapone (IC_{50} = 18.4 ± 3.6 μM) and tolcapone (IC_{50} = 32.5 ± 3.3 μM).

Transport of COMT inhibitors across MDCK II, MDCK-MDR1 and MDCK-BCRP monolayers

The assessment of monolayer integrity was carried out through the monitorization of TEER and Papp determination of the paracellular marker Na-F. These parameters ensure that the established model is adequate for drug permeation studies by presenting sufficiently restrictive tight junctions that impede paracellular permeation, identically to the *in vivo* situation (Abbott *et al.*, 2014). Although registered TEER values were approximately 100 $\Omega.cm^2$ for all cell lines, which could be interpreted as an indicator of leaky monolayers, MDCK II cells are known to display low TEER values (Dukes *et al.*, 2011) due to ion movement through ion pores (Hellinger *et al.*, 2012). Thus, low TEER

does not necessarily imply disturbed paracellular pathways if there is integrity for paracellular marker molecules. Small tracer molecules, such as Na-F are suggested to be used to assess the paracellular permeability of tighter layers (Abbott *et al.*, 2014). Herein, the Papp of Na-F was inferior to $1.0x10^{-6}$ cm/s in MDCK II cells and $0.5x10^{-6}$ cm/s in MDCK-MDR1 and MDCK-BCRP cells (Table 1), supporting the formation of a discriminatory cell monolayer. Papp values below $1\text{-}2x10^{-6}$ cm/s are indicative of monolayer intactness (Ehlers *et al.*, 2014). Another estimated parameter in this assay was mass balance, which was between 80–100 % for less lipophilic compounds and 70–80 % for more lipophilic compounds.

The concentration of donor solutions and the sampling time of each reference and test compound were defined following preliminary assays and considering the sensitivity of the analytical methods, as well as the data from cell viability and stability studies. Prior to transport studies with COMT inhibitors, a set of seven chemically diversified commercial drugs was used to validate experimental conditions (Table 1). Net flux ratios of respective P-gp and BCRP substrates were superior to 2 which verify a correct identification by the respective transporter, and the achieved results were consistent with literature data, demonstrating that the applied method provides enough sensitivity for the identification of P-gp and BCRP substrates.

Among the tested COMT inhibitors, BIA 9-1079 was identified as P-gp substrate (Table 2) with a net flux ratio reduced more than 50 % by verapamil (78.7 ± 10.3 %), attesting the specificity of P-gp mediated efflux. In parallel, BIA 9-1059, entacapone, nebicapone and opicapone were, for the first time, identified as BCRP substrates. After pre-incubation with Ko143, a decrease in net flux ratio of 89.7 ± 2.18 % was obtained for BIA 9-1059, 91.1 ± 2.47 % for entacapone, 64.2 ± 3.96 % for nebicapone and 91.2 ± 1.90 % for opicapone. The detection of net flux ratios higher than 2 together with a

reduction of over 50 % in the presence of an inhibitor, ascertain the identification of COMT inhibitors as P-gp and/or BCRP substrates in accordance to the decision-trees provided by the ITC and FDA (Giacomini *et al.*, 2010; Food and Drug Administration, 2012).

Binding of BIA 9-1079 and tolcapone to plasma and brain tissue

The obtained values of $f_{u,plasma}$ and $f_{u,brain}$ for BIA 9-1079 and tolcapone following ultrafiltration are indicated in Table 3. Both COMT inhibitors revealed high binding to plasma proteins in *in vitro* conditions, with recoveries ranging from 86.1 ± 1.8 % (BIA 9-1079) to 96.0 ± 10.6 % (tolcapone) and stability values of 105.9 ± 3.0 % and 102.2 ± 2.5 %, respectively. Uncorrected and corrected $f_{u,brain}$ values were lower for BIA 9-1079 than tolcapone with recoveries between 97.3 ± 3.1 % for BIA 9-1079 and 91.9 ± 3.07 % for tolcapone. Stability values were 100.2 ± 5.0 % and 86.0 ± 1.4 % for BIA 9-1079 and tolcapone.

Plasma and brain pharmacokinetics of BIA 9-1079 and tolcapone

The mean concentration-time profiles of BIA 9-1079 and tolcapone in plasma and brain, after a single intravenous dose (10 mg/kg) to rats are depicted in Fig. 4A-B. The main pharmacokinetic parameters estimated by non-compartmental analysis and other pharmacokinetic parameters relative to the extent and intra-brain distribution are presented in Table 3. Considering the pharmacokinetic profiles of both compounds in plasma (Fig. 4A), it is visible that the systemic exposure of BIA 9-1079 is greater than that of tolcapone, as corroborated by the $AUC_{0\text{-}inf}$ which was 2.3-fold higher for BIA 9-1079. The 4.0-fold higher $t_{1/2el}$ (5.39 h vs. 1.36 h) demonstrates that BIA 9-1079 was

more slowly eliminated and remained longer in plasma than tolcapone (2.46 h vs. 1.09 h).

In opposition, brain exposure was 3.3-fold higher for tolcapone than for BIA 9-1079, considering the AUC_{0-t} values. The C_{max} in the brain was also 2.1-fold higher for tolcapone and reached almost immediately after administration (0.03 h). Nonetheless, the obtained $K_{p,uu}$ values were below unit for both compounds, indicating a restricted extent of brain penetration and dominant active efflux processes. As previously mentioned, this parameter was determined from K_p and *in vitro* $f_{u,brain}$ converted to $f_{u,brain,corrected}$ according to Fridén et al. (Fridén *et al.*, 2011). In order to determine $f_{u,brain,corrected}$, it was required to estimate $K_{p,uu,cell,pred}$ taking into account the pKa of the drug. Despite possessing two pKa values (4.9 and 10.2 for BIA 9-1079; 3.1 and 9.9 for tolcapone), both compounds were herein considered acids, due to the net negative charge displayed at pH 7.4. The observed $K_{p,uu,cell,pred}$ values (Table 3) reflect a low intracellular accumulation of the compounds and exclude trapping in lysosomes, as well as, uptake into cells. From $f_{u,brain,corrected}$ and $V_{u,brain,pred}$ ($= 1/f_{u,brain,corrected}$) it is noticeable that both compounds reveal non-specific binding to brain parenchyma ($V_{u,brain,pred} > 0.8$ mL/g brain), although this is more evident for BIA 9-1079 than tolcapone, because tolcapone displays a higher $f_{u,brain,corrected}$ (0.247) and it is therefore, more available for target engagement than BIA 9-1079. Brain tissue binding is also influenced by lipophilicity and even though both compounds are moderately lipophilic, BIA 9-1079 is more lipophilic (log D pH 7.4 = 1.7) than tolcapone (log D pH 7.4 = 0.1), originating a higher affinity of BIA 9-1079 to brain components.

The effect of the co-administration of elacridar on the plasma and brain concentration-time profiles of tolcapone and BIA 9-1079 are depicted in Fig. 4C-F. The proximity evidenced in Fig. 4C and 4E between plasma concentrations after vehicle or elacridar

administration and the AUC_{0-t} values of BIA 9-1079 or tolcapone with vehicle or with elacridar (Table 4) suggests that plasma exposure was not affected by the co-administration of elacridar. Nevertheless, statistically significant differences were found in brain concentrations of BIA 9-1079 and tolcapone between elacridar and vehicle-administered rats, namely at 0.25, 0.5 and 1 h post-dosing (Fig. 4D/4F). With elacridar, the brain AUC_{0-t} of BIA 9-1079 and tolcapone increased 2.57- and 2.38-fold, respectively. These results attest the contribution of P-gp and/or BCRP to the limited extent of brain distribution of these COMT inhibitors.

Discussion

The BBB is a dynamic interface responsible for the homeostasis of the CNS through the regulation of the molecular exchanges between the blood and the neural tissue. Its complex microenvironment creates a severely restricted traffic of molecules into the CNS and makes the evaluation of CNS exposure during drug development a very challenging task. This assessment encompasses not only the rate of drug transport across the BBB, but also the extent of equilibration of unbound drug and intra-brain distribution. Using *in vitro* models, it is possible to investigate the permeability of compounds early on, as well as, the interactions with efflux transporters that affect their extent of CNS penetration *in vivo*, namely P-gp and BCRP. Despite having different morphological characteristics from brain endothelial cells, MDCK cells and transfected subclones have been widely used to study permeability and efflux liabilities mediated by the main efflux transporters of the BBB, P-gp and BCRP. In addition to displaying BBB-like permeability, these cells effectively identify a great number of efflux substrates (Garberg *et al.*, 2005; Hellinger *et al.*, 2012). Indeed, bidirectional transport assays with MDCK-MDR1 cells have been reported as a valuable *in vitro* assay to

evaluate human P-gp interactions with compounds targeted to treat CNS disorders (Feng *et al.*, 2008) and these systems are recommended by the ITC to investigate if active efflux by these transporters prevents a compound from crossing the BBB (Brouwer *et al.*, 2013). Therefore, the MDCK II, MDCK-MDR1 and MDCK-BCRP cell lines were selected to examine the influence of P-gp and BCRP on the access of COMT inhibitors to the CNS. Another aspect that was investigated *in vitro* was whether these compounds could inhibit the P-gp or BCRP-mediated efflux of known fluorescent probe substrates (rhodamine-123 and Hoechst 33342).

In the intracellular accumulation assay, reference P-gp (verapamil) and BCRP (Ko143) inhibitors successfully prevented the efflux of rhodamine-123 or Hoescht 33342 in MDCK-MDR1 and MDCK-BCRP cells, respectively. Care was taken to use Ko143 at 0.5 μM in all assays, due to the recently reported lack of BCRP specificity for concentrations above 1 μM (Weidner *et al.*, 2015). Among COMT inhibitors, BIA 9-1079, nebicapone and tolcapone demonstrated a concentration-dependent inhibition of BCRP and IC_{50} values indicate that BIA 9-1079 was the most potent BCRP inhibitor among the test compounds. However, the observed inhibitory effect was not considered clinically relevant and a DDI risk at the BBB is low, as the circulating levels of this compound are 30 times lower in plasma than the reported concentrations that result in inhibition of BCRP. According to Almeida et al. (Almeida *et al.*, 2013) the maximum concentration obtained in plasma for BIA 9-1079 after a single therapeutic oral dose of 50 mg/person of opicapone was 51 ng/mL, while the IC_{50} herein found was 3.85 μM (approximately 1530 ng/mL). So far, the most potent inhibitors capable of affecting efflux at the BBB in humans and non-human primates are tariquidar and elacridar (Bauer *et al.*, 2013, 2016; Montesinos *et al.*, 2014; Tournier *et al.*, 2017), nevertheless these inhibitors are only available for research. For marketed drugs, modulation of

efflux at the BBB is deemed improbable, because the unbound systemic concentrations attained at therapeutic doses are low, meaning that major increases in brain uptake are not usually observed in the presence of clinically relevant doses of the inhibitor (Kalvass *et al.*, 2013).

In transcellular permeability assays, it was possible to identify one P-gp substrate (BIA 9-1079) and four BCRP substrates (BIA 9-1059, entacapone, nebicapone and opicapone) among COMT inhibitors. Notwithstanding, the contribution of P-gp and BCRP-mediated efflux to the overall distribution of compounds across the BBB should be conjugated with information regarding other aspects that affect CNS exposure and/or activity *in vivo*.

Thereby, BIA 9-1079 and tolcapone were herein administered to Wistar rats and the pharmacokinetic parameters obtained in the brain support that both compounds crossed the BBB quickly and soon achieved C_{max}. This is in accordance with their high $P_{appA\text{-}B}$ values attained *in vitro*. Still, the most clinically relevant parameter $K_{p,uu}$ revealed a low extent of brain penetration for both compounds, in particular for BIA 9-1079. These results were not surprising for BIA 9-1079 given that it had been identified as a P-gp substrate *in vitro*. Notwithstanding, tolcapone was not identified *in vitro* as P-gp or BCRP substrate, probably because its very high permeability masked its efflux transport. In fact, this has also been observed for other high permeability efflux substrates, such as verapamil, meaning that the involved efflux transporter(s) was or were unable to cope with compound permeation (Hellinger *et al.*, 2012). This is a limitation of the bidirectional transport assay that may prevent compounds with a $Papp_{AP\text{-}BL}$ close to or higher than $30x10^{-6}$ cm/s from being identified as efflux substrates (Polli *et al.*, 2001; Gameiro *et al.*, 2017), emphasizing the importance of performing *in vivo* studies for such compounds. Even though nebicapone displayed a similarly high

passive permeability, the Papp values for tolcapone were consistently higher in all cell lines and in both directions, suggesting that BCRP was still able to compensate inward flux and identify nebicapone as efflux substrate.

Additionally, the significant increase of brain exposure of BIA 9-1079 and tolcapone following the co-administration with elacridar confirms that P-gp and/or BCRP contribute to their limited access to the brain. Although other authors have reported low total or unbound brain-plasma ratios for tolcapone (Mannisto and Kaakkola, 1999; Forsberg *et al.*, 2003; Hakkarainen *et al.*, 2010), this drug is a known peripheral and central COMT inhibitor, which could misleadingly convey that it crosses the BBB to great extent. In fact, 99 % of brain COMT was inhibited after 0.5 h of an oral administration of tolcapone (30 mg/kg) to Wistar rats (Learmonth *et al.*, 2002) probably due to its elevated potency, as evidenced by the very low IC_{50} values determined for membrane-bound (2 nM) and cytosolic (3 nM) brain COMT (Vieira-Coelho and Soares-da-Silva, 1999). Hence, even though P-gp and BCRP severely hamper drug access to the CNS, efflux substrates can be centrally active if the administered dose is sufficient to result in pharmacologically active concentrations in the CNS. This also occurs with other COMT inhibitors such as nebicapone, which can cause peripheral and central COMT inhibition *in vivo*, despite having been herein identified as BCRP substrate. Nebicapone displays a dose-dependent central COMT inhibitory effect, as a peripheral selectivity is observed at 3 mg/kg but lost at 30 mg/kg following an oral administration in Wistar rats (Parada and Soares-da-Silva, 2003).

Comparatively, BIA 9-1079 crossed the BBB in even less extent than tolcapone (35-fold lower $K_{p,uu}$), meaning that peripheral effects are favoured and CNS effects are much less probable. Indeed, the likelihood of CNS activity of a compound diminishes, as $K_{p,uu}$ decreases (Hammarlund-Udenaes, 2009). Furthermore, despite demonstrating

peripheral selectivity and being a major metabolite of opicapone in animals, the contribution of BIA 9-1079 to the peripheral therapeutic effects of opicapone in humans is considered minor, given that BIA 9-1079 represents less than 20 % of its systemic exposure (Rocha *et al.*, 2013).

In conclusion, using *in vitro* assays with MDCK II, MDCK-MDR1 and MDCK-BCRP cells it was possible to successfully identify P-gp and BCRP inhibitors and substrates among COMT inhibitors. To the best of our knowledge, there are no published *in vitro* studies characterizing the role of P-gp and BCRP on the BBB transport of the tested COMT inhibitors up to date. *In vivo* assays were performed for BIA 9-1079 and tolcapone, providing relevant information in regard to their extent of brain distribution and intra-brain tissue binding. Our studies are in line with the current notion that a conjugation of data from different parameters of CNS penetration is necessary to evaluate and explain brain drug transport.

Authorship Contributions

Participated in research design: Bicker, Fortuna, Alves, Falcão

Conducted experiments: Bicker, Fortuna

Contributed new reagents or analytic tools: Soares-da-Silva

Performed data analysis: Bicker, Fortuna, Alves, Soares-da-Silva, Falcão

Wrote or contributed to the writing of the manuscript: Bicker, Fortuna, Alves, Soares-da-Silva, Falcão

References

Abbott NJ, Dolman DEM, Yusof SR, and Reichel A (2014) Chapter 6. In vitro models of CNS barriers, in *Drug Delivery to the Brain: Physiological Concepts, Methodologies and Approaches* (Hammarlund-Udenaes M et al. eds) pp 163–197, Springer-Verlag New York.

Agarwal S, Hartz AMS, Elmquist WF, and Bauer B (2011) Breast cancer resistance protein and P-glycoprotein in brain cancer: two gatekeepers team up. *Curr Pharm Des* **17**:2793–2802.

Almeida L, Rocha JF, Falcão A, Nuno Palma P, Loureiro AI, Pinto R, Bonifácio MJ, Wright LC, Nunes T, and Soares-da-Silva P (2013) Pharmacokinetics, pharmacodynamics and tolerability of opicapone, a novel catechol-o-methyltransferase inhibitor, in healthy subjects: prediction of slow enzyme-inhibitor complex dissociation of a short-living and very long-acting inhibitor. *Clin Pharmacokinet* **52**:139–151.

Annus Á, and Vécsei L (2017) Spotlight on opicapone as an adjunct to levodopa in Parkinson's disease : design, development and potential place in therapy. *Drug Des Devel Ther* **11**:143–151.

Bauer M, Karch R, Zeitlinger M, Stanek J, and Philippe C (2013) Interaction of 11C-tariquidar and 11C-elacridar with P-glycoprotein and breast cancer resistance protein at the human blood-brain barrier. *J Nucl Med* **54**:1–19.

Bauer M, Römermann K, Karch R, Wulkersdorfer B, Stanek J, Philippe C, Maier-Salamon A, Haslacher H, Jungbauer C, Wadsak W, Jäger W, Löscher W, Hacker M, Zeitlinger M, and Langer O (2016) Pilot PET study to assess the functional interplay between ABCB1 and ABCG2 at the human blood–brain barrier. *Clin Pharmacol Ther* **100**:131–141.

Bicker J, Alves G, Fortuna A, and Falcão A (2014) Blood-brain barrier models and their relevance for a successful development of CNS drug delivery systems: a review. *Eur J Pharm Biopharm* **87**:409–432.

Bonifácio MJ, Sutcliffe JS, Torrão L, Wright LC, and Soares-da-Silva P (2014) Brain and peripheral pharmacokinetics of levodopa in the cynomolgus monkey following administration of opicapone, a third generation nitrocatechol COMT inhibitor. *Neuropharmacology* **77**:334–341.

Brouwer KLR, Keppler D, Hoffmaster KA, Bow DAJ, Cheng Y, Lai Y, Palm JE, Stieger B, and Evers R (2013) In vitro methods to support transporter evaluation in drug discovery and development. *Clin Pharmacol Ther* **94**:95–112.

Bungay P, Bagal S, and Pike A (2015) Chapter 20. Designing peripheral drugs for minimal brain exposure, in *Blood-brain barrier in drug discovery* (Di L, and Kerns EH eds) pp 446–462, John Wiley & Sons, Inc.

Chen Z-Z, Lu Y, Du S-Y, Shang K-X, and Cai C-B (2013) Influence of borneol and muscone on geniposide transport through MDCK and MDCK-MDR1 cells as blood-brain barrier in vitro model. *Int J Pharm* **456**:1–7.

Cole S, Bagal S, El-Kattan A, Fenner K, Hay T, Kempshall S, Lunn G, Varma M, Stupple P, and Speed W (2012) Full efficacy with no CNS side-effects: unachievable panacea or reality? DMPK considerations in design of drugs with limited brain penetration. *Xenobiotica* **42**:11–27.

Di L, Rong H, and Feng B (2013) Demystifying brain penetration in central nervous system drug discovery. *J Med Chem* **56**:2–12.

Dukes JD, Whitley P, and Chalmers AD (2011) The MDCK variety pack: choosing the right strain. *BMC Cell Biol* **12**:43.

Ehlers A, These A, Hessel S, Preiss-Weigert A, and Lampen A (2014) Active

elimination of the marine biotoxin okadaic acid by P-glycoprotein through an in vitro gastrointestinal barrier. *Toxicol Lett* **225**:311–317.

European Medicines Agency (2012) Guideline on the investigation of drug interactions. *CPMP/EWP/560/95/Rev 1 Corr** 1–59.

Feng B, Mills JB, Davidson RE, Mireles RJ, Janiszewski JS, Troutman MD, and Morais SM (2008) In vitro P-glycoprotein assays to predict the in vivo interactions of P-glycoprotein with drugs in the central nervous system. *Drug Metab Dispos* **36**:268–275.

Food and Drug Administration (2012) Guidance for industry: drug interaction studies - study design, data analysis, implications for dosing, and labeling recommendations. 1–79.

Forsberg M, Lehtonen M, Heikkinen M, Savolainen J, Arvinen TJ, Pharmacology D, Toxicology MF, and L PCM (2003) Pharmacokinetics and pharmacodynamics of entacapone and tolcapone after acute and repeated administration: a comparative study in the rat. *J Pharmacol Exp Ther* **304**:498–506.

Fortuna A, Alves G, Soares-da-Silva P, and Falcão A (2013) Pharmacokinetics, brain distribution and plasma protein binding of carbamazepine and nine derivatives: New set of data for predictive in silico ADME models. *Epilepsy Res* **107**:37–50.

Fridén M, Bergström F, Wan H, Rehngren M, Ahlin G, Hammarlund-Udenaes M, and Bredberg U (2011) Measurement of unbound drug exposure in brain: modeling of pH partitioning explains diverging results between the brain slice and brain homogenate methods. *Drug Metab Dispos* **39**:353–362.

Funaki T, Onodera H, Ushiyama N, Tsukamoto Y, Tagami C, Fukazawa H, and Kurama I (1994) The disposition of the tolcapone 3-O-methylated metabolite is affected by the route of administration. *J Pharm Pharmacol* **46**:571–574.

Gameiro M, Silva R, Rocha-Pereira C, Carmo H, Carvalho F, de Lourdes Bastos M, and Remião F (2017) Cellular models and in vitro assays for the screening of modulators of P-gp, MRP1 and BCRP. *Molecules* **22**:1–48.

Garberg P, Ball M, Borg N, Cecchelli R, Fenart L, Hurst RD, Lindmark T, Mabondzo A, Nilsson JE, Raub TJ, Stanimirovic D, Terasaki T, Öberg JO, and Österberg T (2005) In vitro models for the blood-brain barrier. *Toxicol Vitr* **19**:299–334.

Giacomini KM, Huang S, DJ T, Benet LZ, Brouwer KL, Chu X, Dahlin A, Evers R, Fischer V, Hillgren KM, Hoffmaster KA, Ishikawa T, Keppler D, Kim RB, Lee CA, Niemi M, Polli JW, Sugiyama Y, Swaan PW, Ware JA, Wright SH, Yee SW, Zamek-Gliszczynski MJ, and Zhang L (2010) Membrane transporters in drug development. *Nat Rev Drug Discov* **9**:215–236.

Gonçalves D, Alves G, Fortuna A, Soares-da-Silva P, and Falcão A (2013) An HPLC-DAD method for the simultaneous quantification of opicapone (BIA 9-1067) and its active metabolite in human plasma. *Analyst* **138**:2463–2469.

Gonçalves D, Alves G, Fortuna A, Soares-da-Silva P, and Falcão A (2016) Development of a liquid chromatography assay for the determination of opicapone and BIA 9-1079 in rat matrices. *Biomed Chromatogr* **30**:312–322.

Gonçalves D, Alves G, Soares-da-Silva P, and Falcão A (2012) Bioanalytical chromatographic methods for the determination of catechol-O-methyltransferase inhibitors in rodents and human samples: a review. *Anal Chim Acta* **710**:17–32.

Hakkarainen JJ, Jalkanen AJ, Kääriäinen TM, Keski-Rahkonen P, Venäläinen T, Hokkanen J, Mönkkönen J, Suhonen M, and Forsberg MM (2010) Comparison of in vitro cell models in predicting in vivo brain entry of drugs. *Int J Pharm* **402**:27–36.

Hammarlund-Udenaes M (2009) Active-site concentrations of chemicals - are they a

better predictor of effect than plasma/organ/tissue concentrations? *Basic Clin Pharmacol Toxicol* **106**:215–220.

Hammarlund-Udenaes M (2014) Chapter 5. Pharmacokinetic concepts in brain drug delivery, in *Drug delivery to the brain: physiological concepts, methodologies and approaches* (Hammarlund-Udenaes M et al. eds) pp 127–161, Springer-Verlag New York, New York.

Hellinger É, Veszelka S, Tóth AE, Walter F, Kittel Á, Bakk ML, Tihanyi K, Háda V, Nakagawa S, Dinh Ha Duy T, Niwa M, Deli M, and Vastag M (2012) Comparison of brain capillary endothelial cell-based and epithelial (MDCK-MDR1, Caco-2, and VB-Caco-2) cell-based surrogate blood-brain barrier penetration models. *Eur J Pharm Biopharm* **82**:340–351.

Hu HH, Bian YC, Liu Y, Sheng R, Jiang H Di, Yu LS, Hu YZ, and Zeng S (2014) Evaluation of blood-brain barrier and blood-cerebrospinal fluid barrier permeability of 2-phenoxy-indan-1-one derivatives using in vitro cell models. *Int J Pharm* **460**:101–107.

Hubatsch I, Ragnarsson EGE, and Artursson P (2007) Determination of drug permeability and prediction of drug absorption in Caco-2 monolayers. *Nat Protoc* **2**:2111–2119.

Kalvass JC, Polli JW, Bourdet DL, Feng B, Huang S-M, Liu X, Smith QR, Zhang LK, and Zamek-Gliszczynski MJ (2013) Why clinical modulation of efflux transport at the human blood-brain barrier is unlikely: the ITC evidence-based position. *Clin Pharmacol Ther* **94**:80–94.

Kamiie J, Ohtsuki S, Iwase R, Ohmine K, Katsukura Y, Yanai K, Sekine Y, Uchida Y, Ito S, and Terasaki T (2008) Quantitative atlas of membrane transporter proteins: Development and application of a highly sensitive simultaneous LC/MS/MS

method combined with novel in-silico peptide selection criteria. *Pharm Res* **25**:1469–1483.

Kiss LE, Ferreira HS, and Learmonth DA (2008) Efficient synthesis of 2-(trifluoromethyl) nicotinic acid derivatives from simple fluorinated precursors. *Org Lett* **10**:1835–1837.

Kiss LE, and Soares-da-Silva P (2014) Medicinal chemistry of catechol-O-methyltransferase (COMT) inhibitors and their therapeutic utility. *J Med Chem* **57**:8692–8717.

Learmonth DA, Vieira-coelho MA, Benes J, Alves PC, Borges N, and Freitas AP (2002) Synthesis of 1-(3,4-dihydroxy-5-nitrophenyl)-2-phenyl-ethanone and derivatives as potent and long-acting peripheral inhibitors of catechol-O-methyltransferase. *J Med Chem* **45**:685–695.

Li L, Yao QQ, Xu SY, Hu HH, Shen Q, Tian Y, Pan LY, Zhou H, Jiang H Di, Lu C, Yu LS, and Zeng S (2014) Cyclosporin A affects the bioavailability of ginkgolic acids via inhibition of P-gp and BCRP. *Eur J Pharm Biopharm* **88**:759–767.

Loryan I, Sinha V, Mackie C, Van Peer A, Drinkenburg W, Vermeulen A, Morrison D, Monshouwer M, Heald D, and Hammarlund-Udenaes M (2014) Mechanistic understanding of brain drug disposition to optimize the selection of potential neurotherapeutics in drug discovery. *Pharm Res* **31**:2203–2219.

Löscher W, and Potschka H (2005) Role of drug efflux transporters in the brain for drug disposition and treatment of brain diseases. *Prog Neurobiol* **76**:22–76.

Mahar Doan KM, Humphreys JE, Webster LO, Wring SA, Shampine LJ, Serabjit-Singh CJ, Adkison KK, and Polli JW (2002) Passive permeability and P-glycoprotein-mediated efflux differentiate central nervous system (CNS) and non-CNS marketed drugs. *J Pharmacol Exp Ther* **303**:1029–1037.

Mannisto PT, and Kaakkola S (1999) Catechol-O-methyltransferase (COMT): biochemistry, molecular biology, pharmacology, and clinical efficacy of the new selective COMT inhibitors. *Pharmacol Rev* **51**:593–628.

Montesinos RN, Moulari B, Gromand J, Beduneau A, Lamprecht A, and Pellequer Y (2014) Co-administration of P-glycoprotein modulators on loperamide pharmacokinetics and brain distribution. *Drug Metab Dispos* **42**:700–706.

Napolitano A, Bellini G, Borroni E, Zu G, Bonuccelli U, Zürcher G, and Bonuccelli U (2003) Effects of peripheral and central catechol-O-methyltransferase inhibition on striatal extracellular levels of dopamine: a microdialysis study in freely moving rats. *Park Relat Disord* **9**:145–150.

Parada A, and Soares-da-Silva P (2003) BIA 3-202, a novel catechol-O-methyltransferase inhibitor, reduces the peripheral O-methylation of L-DOPA and enhances its availability to the brain. *Pharmacology* **68**:29–37.

Pavek P, Merino G, Wagenaar E, Bolscher E, Novotna M, Jonker JW, and Schinkel AH (2005) Human breast cancer resistance protein: interactions with steroid drugs, hormones, the dietary carcinogen 2-amino-1-methyl-6-phenylimidazo(4,5-b)pyridine, and transport of cimetidine. *J Pharmacol Exp Ther* **312**:144-152.

Polli JW, Wring SA, Humphreys JE, Huang L, Morgan JB, Webster LO, and Serabjit-Singh CS (2001) Rational use of in vitro P-glycoprotein assays in drug discovery. *J Pharmacol Exp Ther* **299**:620–628.

Reichel A (2014) Chapter 12. Integrated approach to optimizing CNS penetration in drug discovery: from the old to the new paradigm and assessment of drug–transporter interactions, in *Drug delivery to the brain: physiological concepts, methodologies and approaches* (Hammarlund-Udenaes M et al. eds) pp 339–374, Springer-Verlag New York.

Rocha JF, Almeida L, Falcão A, Palma PN, Loureiro AI, Pinto R, Bonifácio MJ, Wright LC, Nunes T, and Soares-da-Silva P (2013) Opicapone: a short lived and very long acting novel catechol-O-methyltransferase inhibitor following multiple dose administration in healthy subjects. *Br J Clin Pharmacol* **76**:763–775.

Römermann K, Helmer R, and Löscher W (2015) The antiepileptic drug lamotrigine is a substrate of mouse and human breast cancer resistance protein (ABCG2). *Neuropharmacology* **93**:7–14.

Shawahna R, Uchida Y, Decleves X, Ohtsuki S, Yousif S, Dauchy S, Jacob A, Chassoux F, Daumas-Duport C, Couraud PO, Terasaki T, and Scherrmann JM (2011) Transcriptomic and quantitative proteomic analysis of transporters and drug metabolizing enzymes in freshly isolated human brain microvessels. *Mol Pharm* **8**:1332–1341.

Silva T, Mohamed T, Shakeri A, Rao PPN, Martínez-Gonzalez L, Pérez DI, Martínez A, Valente MJ, Garrido J, Uriarte E, Serrão P, Soares-da-silva P, Remião F, and Borges F (2016) Development of blood-brain barrier permeable nitrocatechol-based catechol O-methyltransferase inhibitors with reduced potential for hepatotoxicity. *J Med Chem* **59**:7584–7597.

Tournier N, Goutal S, Auvity S, Traxl A, Mairinger S, Wanek T, Helal O, Buvat I, Soussan M, and Caillé F (2017) Strategies to inhibit ABCB1- and ABCG2-mediated efflux transport of erlotinib at the blood-brain barrier: a PET study in non-human primates. *J Nucl Med* **58**:117–122.

Uchida Y, Ohtsuki S, Katsukura Y, Ikeda C, Suzuki T, Kamiie J, and Terasaki T (2011) Quantitative targeted absolute proteomics of human blood-brain barrier transporters and receptors. *J Neurochem* **117**:333–345.

Urquhart BL, Ware JA, Tirona RG, Ho RH, Leake BF, Schwarz UI, Zaher H, Palandra

J, Gregor JC, Dresser GK, and Kim RB (2008) Breast cancer resistance protein (ABCG2) and drug disposition: intestinal expression, polymorphisms and sulfasalazine as an in vivo probe. *Pharmacogenet Genomics* **18**:439-448.

Vieira-Coelho MA, and Soares-da-Silva P (1999) Effects of tolcapone upon soluble and membrane-bound brain and liver catechol-O-methyltransferase. *Brain Res* **821**:69–78.

Wang C, and Williams NS (2013) A mass balance approach for calculation of recovery and binding enables the use of ultrafiltration as a rapid method for measurement of plasma protein binding for even highly lipophilic compounds. *J Pharm Biomed Anal* **75**:112–117.

Wang Q, Rager JD, Weinstein K, Kardos PS, Dobson GL, Li J, and Hidalgo IJ (2005) Evaluation of the MDR-MDCK cell line as a permeability screen for the blood-brain barrier. *Int J Pharm* **288**:349–359.

Weidner LD, Zoghbi SS, Lu S, Shukla S, Ambudkar S V, Pike VW, Mulder J, Gottesman MM, Innis RB, and Hall MD (2015) The inhibitor Ko143 is not specific for ABCG2. *J Pharmacol Exp Ther* **354**:384–393.

Footnotes

This work was funded by FEDER funds through the Operational Programme Competitiveness Factors – COMPETE, national funds by FCT - Foundation for Science and Technology under the project [SFRH/BD/78256/2011] and was also supported by BIAL-Portela & Ca S.A.

DMD Fast Forward. Published on September 15, 2017 as DOI: 10.1124/dmd.117.077883
This article has not been copyedited and formatted. The final version may differ from this version.

Figure Legends

Fig. 1. Chemical structures of the analysed COMT inhibitors.

Fig. 2. Intracellular accumulation of rhodamine-123 and Hoechst 33342 in MDCK II, MDCK-MDR1 and MDCK-BCRP cells. (A to B) Demonstration of P-gp and BCRP functionality after a 30 min incubation period with 100 µM verapamil (A) or 0.5 µM Ko143 (B) as positive controls. (C to D) Intracellular uptake observed following a 30 min incubation period with 100 µM test compounds in MDCK-MDR1 (C) and MDCK-BCRP (D) cells. Data compared with negative control cells (no inhibitor) and expressed as mean ± SD ($n = 3$). *$p < 0.05$, **$p < 0.01$ and ***$p < 0.001$.

Fig. 3. Dose-dependent inhibition of BCRP-mediated accumulation of Hoechst 33342 by BIA 9-1079 (A), nebicapone (B) and tolcapone (C) in MDCK-BCRP cells. Values represent mean ± SD ($n = 3$).

Fig. 4. Mean concentration-time profiles of BIA 9-1079 and tolcapone in plasma (A) and brain (B) following 10 mg/kg intravenous administration to Wistar rats. Each data point is presented as mean ± SEM ($n = 27 – 30$ animals per group). The mean concentration-time profiles of BIA 9-1079 and tolcapone in plasma (C and E) and brain (D and F) with and without the co-administration of elacridar (2.5 mg/kg) are depicted. Each data point is presented as mean ± SEM ($n = 8 – 12$ animals per group) and significant differences between group concentrations at specific time-points were calculated by two-tailed Student's t-test. *$p < 0.05$, **$p < 0.01$.

Table 1. Bidirectional apparent permeability coefficient (Papp), efflux ratio (ER) and net flux ratio of reference compounds across MDCK II, MDCK-MDR1 and MDCK-BCRP cell monolayers. Papp values are indicated from the apical to basolateral (AP-BL) and basolateral-to-apical (BL-AP) compartments.

Reference compound	Transport	Donor solution (μM)	MDCK II			MDCK-MDR1			Net flux ratio		MDCK-BCRP			Net flux ratio	
			$Papp_{AP-BL}$ ($x10^{-6}$ cm/s)	$Papp_{BL-AP}$ ($x10^{-6}$ cm/s)	ER	$Papp_{AP-BL}$ ($x10^{-6}$ cm/s)	$Papp_{BL-AP}$ ($x10^{-6}$ cm/s)	ER	Without verapamil	With verapamil	$Papp_{AP-BL}$ ($x10^{-6}$ cm/s)	$Papp_{BL-AP}$ ($x10^{-6}$ cm/s)	ER	Without Ko143	With Ko143
Carbamazepine	PT	10	36.5 (1.93)	19.5 (0.60)	0.53	38.0 (2.54)	20.0 (5.53)	0.53	1.00	-	37.3 (5.60)	19.6 (3.85)	0.53	1.00	-
Propranolol	PT	10	19.6 (4.99)	20.0 (0.16)	1.02	23.8 (2.69)	20.8 (1.51)	0.87	0.85	-	25.4 (2.51)	22.4 (0.59)	0.88	0.86	-
Trazodone	PT	10	38.5 (3.30)	29.4 (1.31)	0.76	33.0 (2.58)	40.4 (3.14)	1.22	1.61	-	37.5 (5.03)	27.4 (2.91)	0.73	0.96	-
Atenolol	PP	100	0.22 (0.06)	0.28 (0.03)	1.27	0.35 (0.14)	0.24 (0.04)	0.69	0.54	-	0.14 (0.11)	0.20 (0.03)	1.43	1.13	-
Cimetidine	Efflux[a]	30	0.56 (0.14)	0.43 (0.03)	0.75	0.06 (0.02)	0.41 (0.05)	**6.40**	**8.50**	0.89	0.15 (0.04)	1.25 (0.08)	**8.34**	**11.1**	1.47
Quinidine	Efflux[b]	10	9.52 (2.53)	12.5 (2.49)	1.31	3.77 (0.91)	29.1 (1.37)	**7.73**	**5.90**	1.13	12.0 (3.48)	15.0 (0.48)	1.25	0.95	-
Sulfasalazine	Efflux[c]	60	0.81 (0.30)	0.28 (0.05)	0.34	0.30 (0.14)	0.17 (0.09)	0.56	1.64	-	0.13 (0.11)	0.30 (0.05)	**2.31**	**6.79**	0.92
Na-F	PP	100	0.48 (0.09)	-	-	0.09 (0.08)	-	-	-	-	0.11 (0.04)	-	-	-	-

[a] Efflux mediated by P-gp and BCRP.

[b] Efflux mediated by P-gp.

[c] Efflux mediated by BCRP.

Na-F, sodium fluorescein; PT, passive transcellular; PP, Passive paracellular. Efflux ratios (ER) and net flux ratios greater than 2 are marked in bold. Papp values are indicated from the apical to basolateral (AP-BL) and basolateral-to-apical (BL-AP) compartments and expressed as mean (SD) (n = 3). Transport classification according to Mahar Doan et al., 2002; Pavek et al., 2005; Wang et al., 2005; Feng et al., 2008; Urquhart et al., 2008.

Table 2. Apparent permeability coefficient (Papp) values, efflux ratio (ER) and net flux ratio of COMT inhibitors across MDCK II, MDCK-MDR1 and MDCK-BCRP cell monolayers.

Test compound	Donor solution (μM)	MDCK II			MDCK-MDR1			Net flux ratio		MDCK-BCRP			Net flux ratio	
		$Papp_{AP-BL}$ ($x10^{-6}$ cm/s)	$Papp_{BL-AP}$ ($x10^{-6}$ cm/s)	ER	$Papp_{AP-BL}$ ($x10^{-6}$ cm/s)	$Papp_{BL-AP}$ ($x10^{-6}$ cm/s)	ER	Without verapamil	With verapamil	$Papp_{AP-BL}$ ($x10^{-6}$ cm/s)	$Papp_{BL-AP}$ ($x10^{-6}$ cm/s)	ER	Without Ko143	With Ko143
BIA 9-1059	60	1.29 (0.27)	1.47 (0.18)	1.14	1.22 (0.23)	0.35 (0.07)	0.29	0.25	-	0.24 (0.08)	1.69 (0.44)	**7.04**	**6.18**	0.64
BIA 9-1079	10	5.23 (2.75)	8.47 (0.91)	1.62	3.47 (1.77)	15.9 (4.19)	**4.58**	**2.83**	0.60	7.14 (4.63)	13.6 (1.74)	1.90	1.17	-
Entacapone	30	6.33 (0.37)	6.02 (0.39)	0.95	3.51 (1.33)	1.29 (0.36)	0.37	0.39	-	0.98 (0.19)	11.1 (0.92)	**11.3**	**11.9**	1.06
Nebicapone	10	24.6 (1.45)	17.6 (4.18)	0.72	23.9 (7.06)	14.3 (2.60)	0.60	0.83	-	5.40 (0.09)	11.6 (0.63)	**2.15**	**2.99**	1.07
Opicapone	30	4.72 (2.33)	6.08 (0.38)	1.29	2.56 (1.08)	2.50 (0.39)	0.98	0.76	-	0.42 (0.09)	9.73 (1.13)	**23.2**	**18.0**	1.58
Tolcapone	10	26.6 (5.07)	20.6 (3.87)	0.77	24.3 (2.84)	19.5 (3.37)	0.80	1.04	-	28.3 (2.93)	23.7 (1.65)	0.84	1.09	-

Efflux ratios (ER) and net flux ratios greater than 2 are marked in bold. Papp values are indicated from the apical to basolateral (AP-BL) and basolateral-to-apical (BL-AP) compartments and expressed as mean (SD) (n = 3).

Table 3. Pharmacokinetic parameters and binding data of BIA 9-1079 and tolcapone in plasma and brain after intravenous administration (10 mg/kg) to Wistar rats.

		t_{max} (h)	C_{max} (µg/mL)	AUC_{0-t} (µg.h/mL)	AUC_{0-inf} (µg.h/mL)	AUC_{extrap} (%)	K_{el} (/h)	$t_{1/2el}$ (h)	MRT (h)
BIA 9-1079	Plasma	0.03	52.78	84.08	84.94	1.02	0.13	5.39	2.46
	Brain	0.08	0.096	0.017	NC	NC	0.66	1.05	0.23
Tolcapone	Plasma	0.03	67.12	36.24	36.28	0.10	0.51	1.36	1.09
	Brain	0.03	0.205	0.056	0.057	1.79	1.53	0.45	0.38

	K_p	$f_{u,plasma}$	$f_{u,brain}$	$f_{u,brain,corrected}$	$V_{u,brain,pred}$ (mL/g)	$K_{p,uu}$	$K_{p,uu,cyto,pred}$	$K_{p,uu,lyso,pred}$	$K_{p,uu,cell,pred}$
BIA 9-1079	0.0002	0.002 (0.001)	0.008 (0.001)	0.013	79.27	0.001	0.577	0.020	0.656
Tolcapone	0.0015	0.011 (0.003)	0.162 (0.028)	0.247	4.047	0.035	0.575	0.013	0.655

C_{max} is expressed in µg/g and AUC is expressed in µg.h/g in brain tissue; The presented $V_{u,brain,pred}$, $K_{p,uu,cyto,pred}$, $K_{p,uu,lyso,pred}$ and $K_{p,uu,cell,pred}$ values were predicted according to the pH partitioning theory. $f_{u,plasma}$ and $f_{u,brain}$ values are expressed as mean (SD), $n = 4$.

AUC_{extrap}, extrapolated area under the concentration-time curve; AUC_{0-inf}, area under the concentration-time curve from time zero to infinite; AUC_{0-t}, area under the concentration-time curve from time zero to the last measurable concentration; C_{max}, maximum concentration; $f_{u,plasma}$, unbound drug fraction in plasma; $f_{u,brain}$, unbound drug fraction in the brain; K_{el}, apparent elimination rate constant; K_p, ratio of total brain-to-plasma AUC_{0-t}; $K_{p,uu}$, unbound brain-to-plasma ratio; $K_{p,uu,cell,pred}$, predicted unbound drug intracellular-to-extracellular partitioning coefficient; $K_{p,uu,cyto,pred}$, predicted unbound cytosolic-to-extracellular drug concentration ratio; $K_{p,uu,lyso,pred}$,

predicted lysosomic-to-cytosolic unbound drug concentration ratio; MRT, mean residence time; NC, not calculated; $t_{1/2el}$, apparent terminal elimination half-life; t_{max}, time to achieve the maximum concentration; $V_{u,brain,pred,}$ predicted volume of distribution of unbound drug in the brain.

DMD Fast Forward. Published on September 15, 2017 as DOI: 10.1124/dmd.117.077883
This article has not been copyedited and formatted. The final version may differ from this version.

Table 4. Plasma and brain exposure of BIA 9-1079 and tolcapone after intravenous administration (10 mg/kg) to Wistar rats with or without co-administration of elacridar (2.5 mg/kg).

		AUC_{0-t} (µg.h/mL)		K_p		$K_{p,uu}$	
		Vehicle	Elacridar	Vehicle	Elacridar	Vehicle	Elacridar
BIA 9-1079	Plasma	32.71	37.34	0.001	0.003	0.007	0.017
	Brain	0.037	0.095				
Tolcapone	Plasma	27.31	28.59	0.002	0.004	0.041	0.095
	Brain	0.050	0.119				

AUC is expressed in µg.h/g in brain tissue;

AUC_{0-t}, area under the concentration-time curve from time zero to the last measurable concentration; K_p, ratio of total brain-to-plasma AUC_{0-t}; $K_{p,uu}$, unbound brain-to-plasma ratio;

Figure 1

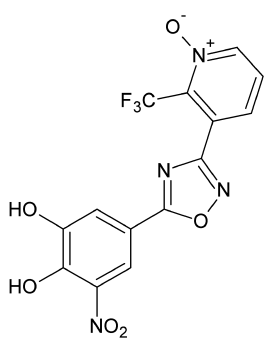

BIA 9-1059

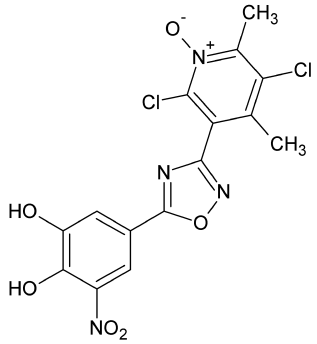

Opicapone

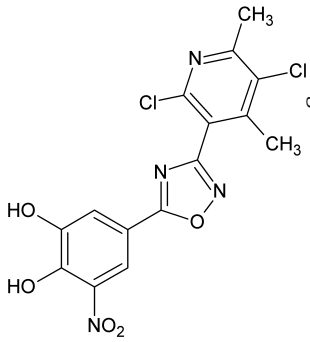

BIA 9-1079

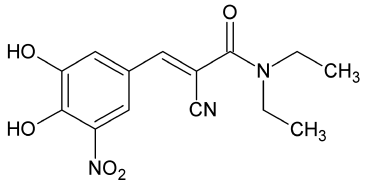

Entacapone

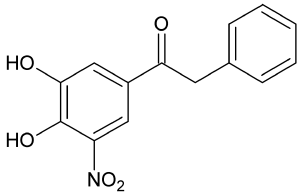

Nebicapone

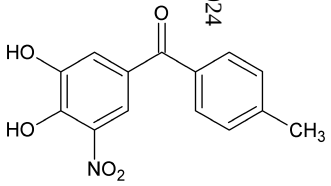

Tolcapone

Figure 2

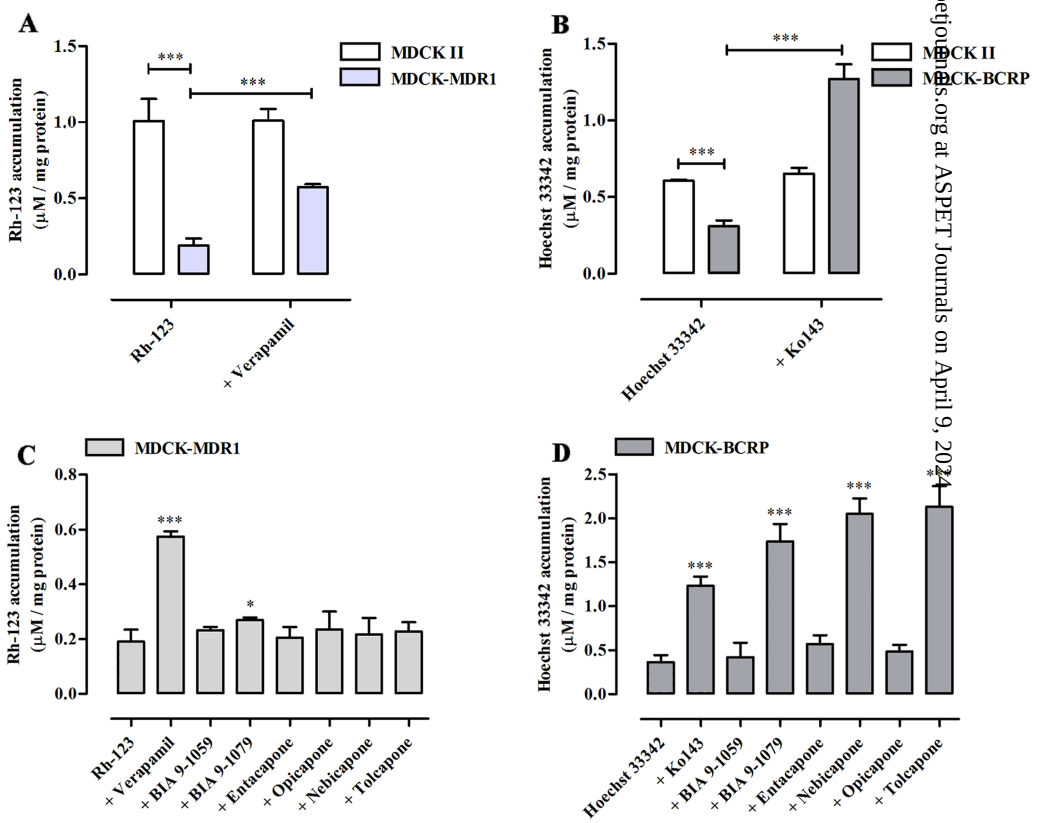

Figure 3

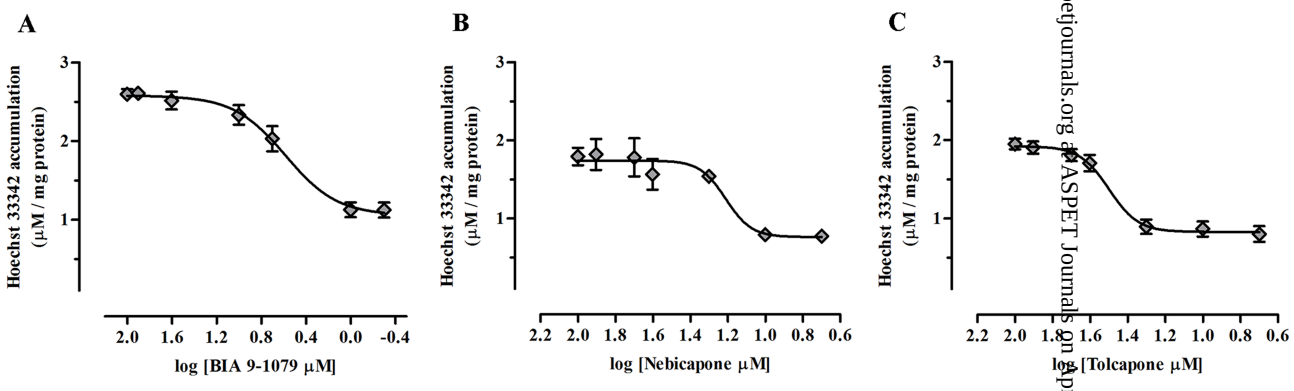

Figure 4